IEEE Journal of Microwaves

Received 9 December 2021; revised 15 February 2022; accepted 17 February 2022. Date of publication 15 March 2022; date of current version 7 April 2022.

Digital Object Identifier 10.1109/JMW.2022.3153690

Radar Scenario Generation for Automotive Applications in the E Band

PATRICK RIPPL (Graduate Student Member, IEEE), JOHANNES IBERLE (Student Member, IEEE), PHILIPP A. SCHARF (Graduate Student Member, IEEE), AND THOMAS WALTER (Member, IEEE)

(Regular Paper)

Laboratory for Microtechnology, University of Applied Sciences Ulm, 89081 Ulm, Germany

CORRESPONDING AUTHOR: Patrick Rippl (e-mail: patrick.rippl@thu.de).

This work was supported by the German Federal Ministry of Education and Research (BMBF) within the project InnoSÜD under Grant 03IHS024B. The article processing charge was funded by the Baden-Württemberg Ministry of Science, Research and Culture and the University of Applied Sciences Ulm in the funding program Open Access Publishing.

ABSTRACT In this publication, a radar scenario generation approach for chirp sequence frequency modulated continuous wave radars simulating targets in the near-range of vehicle surroundings is presented. Key interest is the generation and the replay of arbitrary signals for a CS-FMCW radar by directly modulating the carrier signal. This approach enables the reproduction of traffic scenarios including significant micro-Doppler signatures of traffic participants. In the presented approach, the received E band signal is converted from the RF to an IF band, in which the information about velocity and range of a target is modulated with the usage of an IQ modulator. Since the working principle of the radar target simulator is not based on a delay line, the target profiles can solely be generated on the PC from where they are modulated onto the radar signal via digital-analog conversion. The modulation signals can either be generated in the time or frequency domain which allows an accurate and fast reproduction of real-world scenarios. When generated in the frequency domain, the 2D-IFFT provides an efficient way of transforming commonly used range Doppler maps into the desired modulation signals. This way, range-velocity profiles of complex traffic participants such as pedestrians or cyclists can be generated and simulated in arbitrary circumstances.

INDEX TERMS Automotive radar, frequency modulation, micro-Doppler signatures, millimeter wave radar, radar target simulator.

I. INTRODUCTION

The path towards highly automated and autonomous driving requires a vast amount of sensors in order to be able to observe and monitor the surroundings in traffic scenarios [1], [2]. Considering the future change within the transport habits, smart signal processing as well as machine learning algorithms that enable the classification of the vehicle surroundings will be of high importance in the near future [3]. Since the requirements in terms of reliability and capability of bearing great loads in day-to-day operations in the automotive sector are high [4], it is inevitable to provide reliable sensor systems in order to reach higher automation levels. There is a vast amount of possible traffic scenarios that either are impossible to simulate in the real world (due to risk of injuries) or the variety of the scenarios would require a disproportionate amount of test cycles which would economically be unfeasible. Using a virtual environment, the expenses to test sensors are reduced and thus an easier and cost-effective way of verifying the sensor systems is provided. Therefore, the training of sensor algorithms is facilitated this way.

Radar sensors can be used for the detection of objects in the far range as well as for the close range. A Radar Target Simulator (RTS) provides the possibility to test and validate radar sensor systems. In this approach the focus is set on chirp-sequence frequency modulated continuous waveform (CS-FMCW) radar as it is widely used in the automotive sector. This radar architecture allows for gathering information on the range and velocity of objects within the vehicle surroundings.

There are several concepts that simulate objects in front of the vehicle either for long range or in the near range. The main

TABLE 1. Radar Sensor and Waveform Configuration

f_0	B_c	T_c	T_{RRI}	N_c	f_s
76.5 GHz	1.5 GHz	70 µs	100 µs	255	20 MS/s

difference between the concepts is to either delay the RF signal by transmission lines [5], [6], or digitally [7]. A more flexible architecture is a purely modulation-based RTS [8]–[10]. The RTSs based on modulation provide a more adjustable and more compact solution. Most of these concepts have in common that the modulated signal is freely running and not synchronized with the radar under test (RUT). The system architecture used in this approach includes a synchronization of the RUT and the RTS by using the single radar chirps as trigger inputs for the modulation via the RTS. This way, every single chirp is modulated onto the corresponding frequency chirp of the RUT which ensures a precisely timed transfer of information. In the following work, the generation of targets in the near-range of a RUT will be described.

Since classification of vulnerable road users often times is based on their extracted Micro-Doppler components [11], [12], an example on the simulation of micro-Doppler signatures of vulnerable road users based on a human walking model from [13] and [14] will be given in the end. Since the velocity in CS-FMCW is measured indirectly via a frequency shift, the presented approach also allows for a signal generation purely based on given range-profiles without any velocity information beforehand.

II. WORKING PRINCIPLE

The overall system configuration consists of the RUT and the RTS that is driven by a PC via a digital to analog converter (DAC). At first, the configuration of the RUT will be described. Afterwards, the hardware and software setup with respect to the RTS will be presented.

A. RADAR UNDER TEST

A self-designed sensor, as presented in [12] with a single receiving and a single emitting channel is used as the RUT. The sensor is working in CS-FMCW mode with the configuration settings depicted in Table 1. Since a single receiving channel is used, angular resolution is not possible. An approach concerning angular resolution and RTS scenario generation is shown in [15].

Table 1 depicts f_0 as the center frequency, B_c as chirp bandwidth, T_c as the chirp duration, T_{RRI} as the ramp repetition interval, N_c as the number of chirps per frame used for the following post processing calculations and f_s is both, the ADC and the DAC sampling rate.

The sampling rate of the ADC limits the maximum range to $R_{max} = 70$ m. With this radar configuration, the maximum target velocity $v_{max} = 9.8$ m/s and the range resolution $R_{res} = 0.1$ m is reached. This radar configuration hence allows for a simulation and measurement of micro-Doppler components of vulnerable road users such as pedestrians or cyclists.

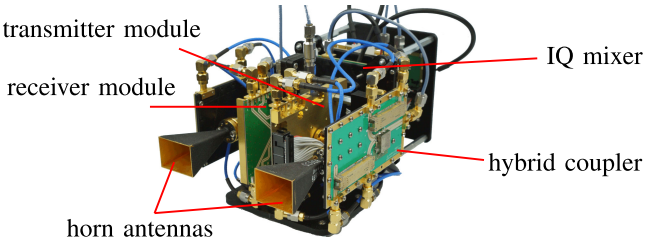

FIGURE 1. RTS used for the radar target replay with labeled main hardware components.

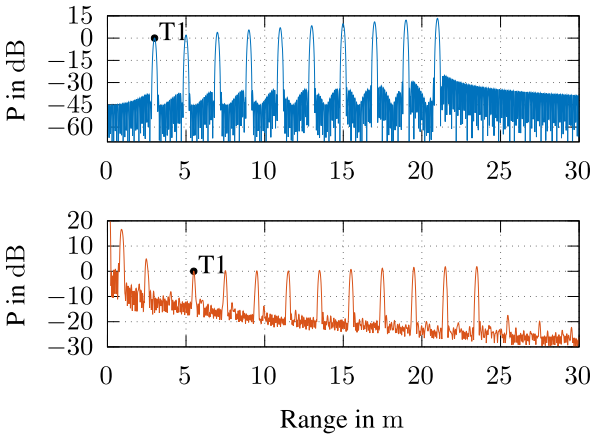

FIGURE 2. Range information of the transmitted RTS signal (top) and of the received RUT signal (bottom). The spectra are normalized with respect to the first generated target T1.

B. RADAR TARGET SIMULATOR

At first, the hardware setup of the RTS depicted in Fig. 1 is shortly summarized. The detailed hardware configuration was already in use for the replay of scenarios for a continuous wave (CW) radar sensor as depicted in [16] and [17] as well as an CS-FMCW approach [9]. Therefore, a more detailed description of the hardware setup can be found in those publications.

For a scenario generation it has to be taken into account that the minimum target range is limited by the free path space of 1 m and the signal delay due to the cable length of 1.5 m. Moreover, an amplitude correction of the transmitted signal s_{Tx} is necessary due to the frequency-dependent behavior of the system.

The required adjustments are exemplary visualized in Fig. 2. Here, the transmitted signal s_{Tx} consists of ten equidistant distributed targets with an increasing signal power to compensate the frequency-dependent attenuation of the hardware setup. On the receiving end, the signal s_{Rx} shows one target at 1 m, which corresponds to the antennas of the RTS and one target at 2.5 m, which corresponds to the signal loss due to the cable length as well as the distance from the radar to the RTS. Subsequently, the modulated desired targets in s_{Rx} are shifted by 2.5 m with an equal amplitude. As mentioned, the ADC sampling rate limits R_{max}. However, assuming targets at different ranges with an equal amplitude, the full scale

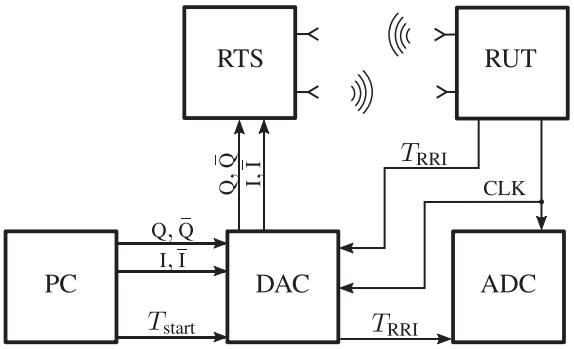

FIGURE 3. Signal flow of the presented system setup.

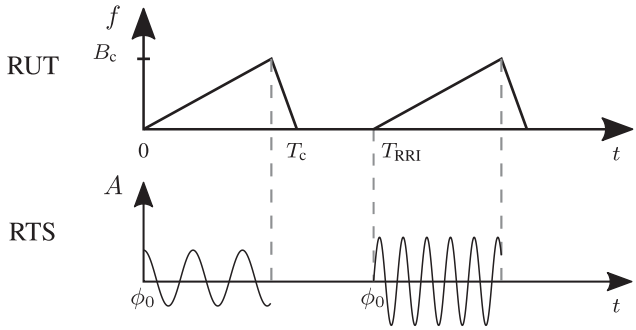

FIGURE 4. Simplified overview of two chirps and the corresponding RTS target response in order to illustrate that every single chirp can be varied in frequency, phase and amplitude and is triggered along with the ramp interval T_{RRI} of the RUT.

output of the DAC is set to the target at the maximum range because of the amplitude compensation depicted in Fig. 2. The DAC amplitudes of the closer targets are then calculated accordingly. Due to this behavior, the maximum range in the following equals 30 m. Consequently, the scope of the scenarios that are generated is the near-field range between 2.5 m to 30 m.

C. SYSTEM SETUP

In order to understand the interaction between the subsystems, Fig. 3 illustrates the simplified block diagram of the system setup. The PC provides differential I and Q signals on IF level for the RTS along with the trigger T_{start}, signaling that the prepared input signal is ready, i.e. loaded into the DAC buffer. This trigger allows for a loop through of T_{RRI} from the RUT to the ADC and thus ensures that the radar signal gets recorded as soon as the RTS sends the generated target response. The raw IF signal of the RUT is sampled with the ADC and locally saved for further signal processing. Furthermore, the RUT sends a trigger signal at every time instance a chirp is transmitted.

Fig. 4 depicts the simplified target generation. As soon as the data transfer from the DAC is ready, the generated chirp modulation signals are sent to the RTS when a frequency ramp is transmitted by the RUT. In this approach the frequencies, as well as the starting phase ϕ_0, within the transmitted chirps can arbitrarily be chosen. This new approach comes with the advantage that the modulated chirp signal does not run freely but instead is triggered for every single chirp. Due to the synchronization of the DAC and RUT clocks, there is no drift and every target signal is fully synchronized with the corresponding radar chirps. Furthermore, since phase and frequency can be set for every chirp, the generation of any target response, i.e. distance and velocity, is possible and is not limited to discrete values. However, the range resolution of the system is limited by the RUT. Even though this procedure is independent of the time between ramps T_{RRI}, the value is still needed for the generation of the range-velocity profiles as it will be shown in the next chapter. By varying the amplitude A_t, different radar cross sections can be simulated. Because DAC and ADC are configured in FIFO mode along with a buffer, the replay of arbitrarily long signals is enabled. Because of the used buffer method, there is a latency for the overall system that depends on the length of the data stream.

III. SIGNAL GENERATION

In the following, the focus for the RTS signals will be set on the generation of the IF signal. In general, a target list containing distance, velocity and amplitude serves as input for the signal generation methods. For the target response generation two approaches will be evaluated and compared. While one approach focuses on the signal generation of every single chirp, the other is based on the information within a frame, i.e. multiple chirps. In the following a frame is defined as consisting of N_c chirps and hence comprises a duration of $T_{frame} = N_c \cdot T_{RRI}$. Hence, the chirp-wise modulation treats each of the chirps independently allowing for maximum flexibility in the radar signal modulation. Frame-wise modulation assumes constant-radial-velocity of all targets within the time of one frame and thus is a more coarse way of reproducing the target information. In conclusion, this means that the input target list that provides the information for the target response is generated by sampling the distance, velocity and RCS of the targets with $1/T_{RRI}$ for the chirp-wise method and with $1/T_{frame}$ for the frame-wise approach. This way, a time-discrete information of the target parameters is generated.

A. CHIRP-WISE MODULATION

In the beginning, the signal generation using the chirp-wise approach will be explained. Since every target response within a single chirp is calculated separately with its starting phase, there is no need for providing the velocity as input. Due to the CS-FMCW properties, the velocity is calculated by the phase shift of the single frequencies that are contained in the generated chirp. Thus, the input target list contains the information of the target ranges R_t and amplitudes A_t at every time step $j \cdot T_{RRI}$. Fig. 5 shows the corresponding times of the chirp-wise signal generation approach. Every row in this matrix corresponds to the target response of one chirp. The number of rows in this matrix hence corresponds to the number of chirps that are generated. The number of columns is set by the chosen sampling period $T_s = 1/f_s$ of the target response. With

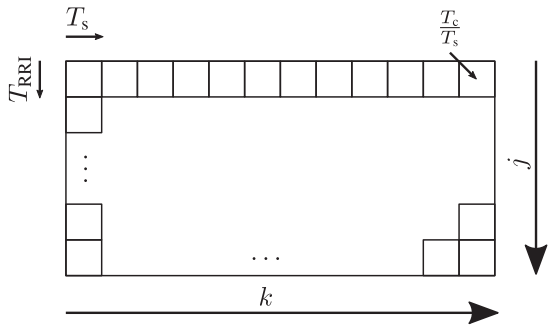

FIGURE 5. $K \times J$ **matrix with** $k = 1 \ldots K$ **and** $j = 1 \ldots J$ **containing the target responses for every chirp along with the corresponding time values.**

the given parameters, a 255×1400 sized matrix that holds the target response amplitudes per sample results for one frame.

Assuming a constant phase shift ϕ_t for the radar signal with the center frequency f_0 and free-space wavelength λ_0 due to the target,

$$\phi_t = \frac{2\pi}{\lambda_0} 2R_t. \tag{1}$$

The IF frequency f_{R_t} corresponding to the range of the target R_t is calculated by

$$f_{R_t} = \frac{2B_c R_t}{T_c c_0} \tag{2}$$

and hence the resulting intermediate signal for the target is

$$s_t(t_c) = A_t \cos(2\pi f_{R_t} \cdot t_c + \phi_t) \tag{3}$$

sampled with the DAC samplerate results in

$$s_t[k] = A_t \cos(2\pi \cdot f_{R_t} \cdot kT_s + \phi_t). \tag{4}$$

The overall signal containing all targets N_t within T_c is then given by

$$s_c[k] = \sum_{t=1}^{N_t} s_t[k]. \tag{5}$$

For this approach, T_{RRI} has to be known in order to generate the input target list since it is needed to sample the target ranges for the target response within the single chirp signals. However, solely for the calculation of the signals, it is not needed. This procedure comes with the advantage that the signals within the generated scenario are independent of each other, i.e. the number of chirps within a frame does not need to be known in advance. Furthermore, a benefit of including ϕ_t is that there is no overweight at one sample, due to the superposition of multiple s_t because slight range differences already cause phase shifts of the modulated signal. In the end, the full scale range of the DAC is set by the maximum signal amplitude and would significantly be decreased if multiple targets start with the same phase.

B. FRAME-WISE MODULATION

In contrast to the generation of the target response for every single chirp, there is the possibility to generate the target response for a multitude of chirps at once. This means, that the input and output of this approach will be frame-discrete. In this method a constant velocity, i.e. phase shift from chirp to chirp, within N_c is assumed. For this approach, N_c has to be known in advance, since the chirps of the following frame will start with a starting phase ϕ_0 again which is not related to the last chirp of the previous frame. With the radar settings shown in Table 1, the frame time $T_{frame} = 25.5\,\text{ms}$. The maximum velocity

$$v_{max} = \frac{1}{4} \frac{c_0}{f_0 \cdot T_{RRI}}, \tag{6}$$

equals $9.8\,\text{m/s}$ and hence a max. progression of target range of $0.25\,\text{m}$ within T_{frame} is possible. Since $R_{res} = 0.1\,\text{m}$, this distance is resolvable with the given radar settings. Thus, the frame-discrete approach will show different results in the corresponding range-Doppler (rD) plots compared to the frame-wise generated scenarios. In order to explain the benefits of this method as well, first the time-domain generation of the signal will be evaluated. Afterwards the focus will be set on the generation of the signals in the frequency domain, which will show the potential of this approach.

For the signal generation, the range as well as the velocity component of the target v_t is needed. In the frame-wise approach the input target list is sampled with $1/T_{frame}$. In general, the intermediate frequency of the signal is calculated by

$$f_{IF_t} = \underbrace{\frac{2BR_t}{c_0 T_c}}_{f_{R_t}} + \underbrace{\frac{2f_c v_t}{c_0}}_{f_{D_t}}, \tag{7}$$

with f_{D_t} as the Doppler frequency. The signal for the target t is then

$$s_t[k, j] = A_t \cos(2\pi (f_{R_t} kT_s + f_{D_t} jT_{RRI})), \tag{8}$$

which results in

$$s_c[k, j] = \sum_{t=1}^{N_t} s_t[k, j]. \tag{9}$$

Attaching every jth chirp leads to the signal of the frame

$$s_{frame}[k] = \left[s_c\left[k, j\right], s_c\left[k, j+1\right], \ldots, s_c\left[k, N_c\right]\right]. \tag{10}$$

This shows that there is a possible phase shift between each frame, since the signal of the following frame is independent of the preceding one.

As an alternative to the generation in the time-domain, the signal can also be calculated using the 2D inverse Fast Fourier Transform (2D-IFFT). Using this method, the calculation time can be decreased significantly due to the efficient implementation of the algorithm.

The result of the discrete inverse Fourier transform x of an $K \times J$ matrix X results in a real-valued matrix, when the vectors in the input matrix X are conjugate symmetric in both dimensions. Thus, X is constructed from an rD map with values corresponding to the target information A_t, R_t and v_t

from the input target list. In order to receive a real-valued result x of the 2D-IFFT, the constructed rD map consists of both, positive and negative range information and is calculated by

$$x_{p,q} = \frac{1}{K}\sum_{k=1}^{K}\frac{1}{J}\sum_{j=1}^{J}\omega_K^{(k-1)(p-1)}\omega_J^{(j-1)(q-1)}X_{k,j}. \quad (11)$$

ω_k and ω_j are complex roots of unity:

$$\omega_K = \exp(2\pi i/K), \quad (12)$$

$$\omega_J = \exp(2\pi i/J), \quad (13)$$

with the imaginary unit i. p runs from 1 to K and q runs from 1 to J. Again, x is a 2 dimensional matrix that is reshaped into a $1 \times KJ$ vector and scaled such that a data stream s_{frame} for the DAC results.

Summarizing, the two frame-wise generation methods are compared with respect to the computational power. First, the 2D-IFFT transforms along r dimension, then along c dimension, which corresponds to the order $O(KJ\log(KJ))$. The only parameter with a significant influence on the computation time is the generation of the input rD map, which depends on the number of targets N_t within the frame and barely costs any computation time. However, the transformation from a given rD map to the corresponding time signal for the RTS is calculated quickly. In the approach based on the time-domain signal generation the order is $O(\text{N}_\text{t})$. That means that the computational effort is linearly increasing with the number of targets within the frame, while it is almost constant with the 2D-IFFT approach.

Another advantage of the 2D-IFFT approach is the reproduction of measurement results. Often times the results of CS-FMCW measurements are processed into an rD plot [3] where proven post processing methods such as CFAR filtering are applied. With the 2D-IFFT approach, this result can easily be used for the RTS. Moreover, the direct transformation of the rD map incorporates the blurring from slight changes within the chirps and hence reproduces range changes within T_RRI.

IV. SCENARIO GENERATION & REPLAY

With the outlined target generation methods, it is possible to synthesize and replay arbitrary scenarios. The following illustration will be focused on the car environment use case, where the focus is set on vulnerable road users in near-range scenarios. For comparison reasons, the chirp-wise and frame-wise approach will be analyzed by means of a target list profile that is extracted from a human walking model, as described in [13]. In the end, the generated signals are replayed with the RTS and recorded by the RUT in an anechoic chamber in order to suppress unwanted targets. In this setup, the distance between the RTS and the radar sensor is 1 m. Real life scenarios are not discrete by any means and thus for the depiction of the human walking model, the resulting rD plot of the chirp-wise approach is depicted in Fig. 6. For the frame evaluation and thus also for the processing of the received radar

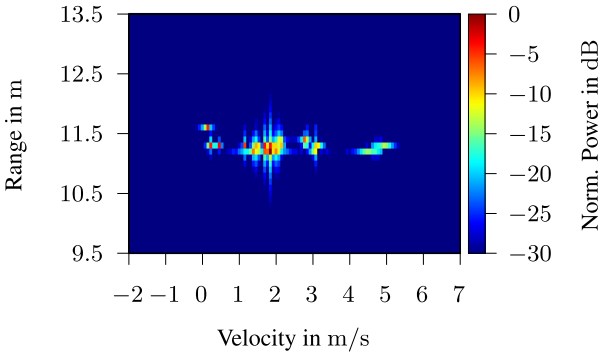

FIGURE 6. rD map calculated by the generated chirps based on the information of the human walking model. This signal serves as input for the RTS.

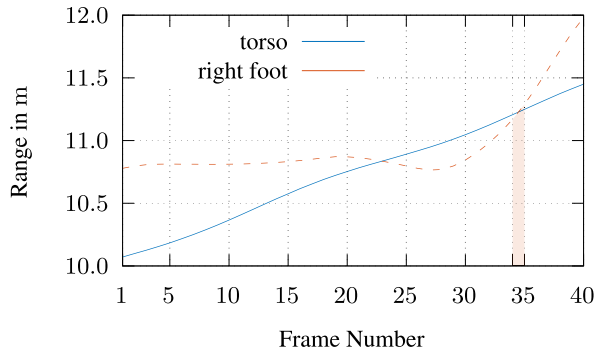

FIGURE 7. Range profile of torso and right foot of the human walking model from [13] with frame of interest 35 highlighted.

chirps since the frame consists of 255 chirps, the radar and processing settings from Table 1 are used. For visualization and comparison reasons, the single body parts are weighted equally and thus do not include RCS information. However, the RCS could be included by varying the signal amplitude. Furthermore, neither a window function nor zero padding is applied. In the frame, the velocity resolution is limited by $N_\text{c} \cdot T_\text{RRI}$. Assuming a target with the max resolvable velocity of 9.8 m/s, its velocity equals 0.98 mm/T_RRI. Thus in T_frame, within 255 chirps, the target will progress 0.25 m which is resolvable in distance in the resulting rD plot.

Fig. 7 depicts the range profile of two significant body parts within the first 1.02 s of the movement, i.e. 40 frames. As depicted, the torso movement produces an approximately constant increasing behavior (within the first 40 frames), while the foot movement exhibits a more complex progression. Even though the torso movement shows great potential for a radar classification approach [12], [18], for now the focus is set on the movement of the right foot. In order to facilitate the evaluation of the two approaches, the movement of the right foot of the simulated person within the time interval 0.8670 s to 0.8925 s is focused in the following. This interval, between frame 34 and 35, is chosen because there is a significant change of range present. Within the duration of this frame, the foot covers a distance from 11.17 m to 11.29 m.

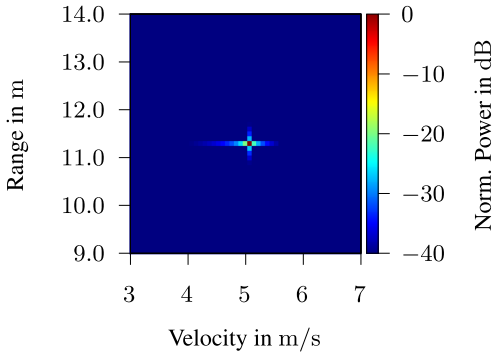

FIGURE 8. rD map of the generated signal of the right foot using the frame-wise signal generation approach.

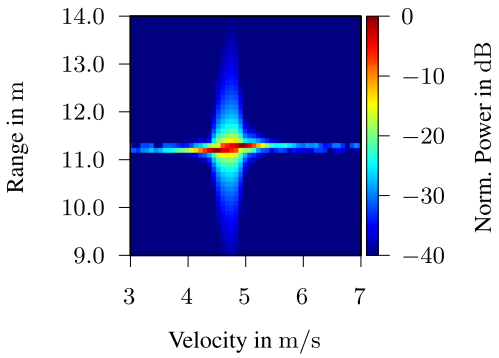

FIGURE 9. rD map of the generated signal of the right foot using the chirp-wise signal generation approach.

For the calculation of the rD maps in Fig. 8 and Fig. 9 neither a window function nor zero padding are applied. Because of the missing interpolation in the frequency-domain, the range resolution is 0.1 m per frequency bin, i.e. per pixel. For the comparison of the two target response generation methods, the foot movement is focused and thus the maps are limited by the according velocity and range intervals and the data is normalized to their respective maximum value.

Using the frame-wise signal generation, one very distinct target at [5.1 m/s, 11.3 m] can be detected. The blurring around this point target is due to the sharp edges of the rectangular window for the 2D-FFT processing. For this frame, the range bin almost corresponds to the desired target range and hence the blurring in range-direction is less pronounced compared to the blurring in velocity-direction.

The rD map of the chirp-wise signal generation approach exhibits a significant blurring in velocity as well as range direction. The generated target lies between 11.1 m to 11.3 m with a velocity of 4.2 m/s to 5.1 m/s. The rD maps point out that the chirp-wise signal generation method enables a more accurate depiction of real world scenarios since the movement within T_{frame} can also be simulated. However, for the replay of measured scenarios instead of simulations, the frame-wise approach using the 2D-IFFT allows for a quick transformation via the corresponding rD maps since these rD maps already

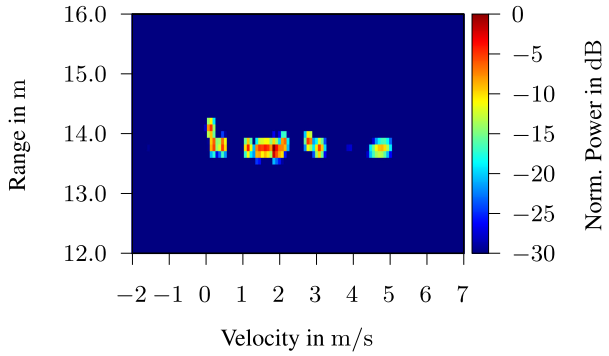

FIGURE 10. rD map of the replayed scenario of human walking model modulated with the chirp-wise approach.

incorporate target progression blurring within the progression of the measured chirp signals.

Because of the described system setup, the single chirps of the radar trigger the activation of the RTS. That means, that every single chirp can thus be modulated onto the corresponding frequency chirp of the RUT. The resulting scenario of the input (Fig. 6) is depicted in Fig. 10. For the generation of this rD map, the signal is highpass filtered in order to remove the static targets due to the RTS. For generating the rD map, a Hanning window is used for the 2D-FFT. Furthermore, the data is normalized to the target with the highest amplitude within this frame. The replayed scenario shows all the target components that were present in the input scenario depicted in Fig. 6. As mentioned, every target in the resulting scenario exhibits an offset of 2.5 m.

In order to evaluate the dynamic performance of the scene generation, the velocity components of the model are shown over time. For the calculation of the following velocity-time plots, a short-time-FFT (STFFT) is performed over the generated target response signals and the received IF signal, respectively. To calculate the result of the STFFT the amplitude of the occurring velocities of each frame is summed for all ranges. By letting the chirps used for the frame evaluation overlap, a higher time resolution is achieved. This way the single bins are not frame-discrete but instead interpolated in time direction.

Fig. 11 depicts the velocity information of the transmitted target response that is modulated onto the radar signal. Thus, this illustration shows the expected result after modulating the scene onto the RUT. In the transmitted signal, the single components of the human walking model are clearly visible without any noise floor. The highest amplitude is be around 0.5 s where some components contain the same velocity and thus coincide in the velocity-time map. For comparison reasons, the plot is normalized to this amplitude.

Fig. 12 depicts the result of the replayed scenario in the velocity-time domain. Due to the radar properties, applying zero-velocity blanking is useful to make the components with a non-zero velocity more visible which allows for a better comparison to the earlier shown input. The amplitudes

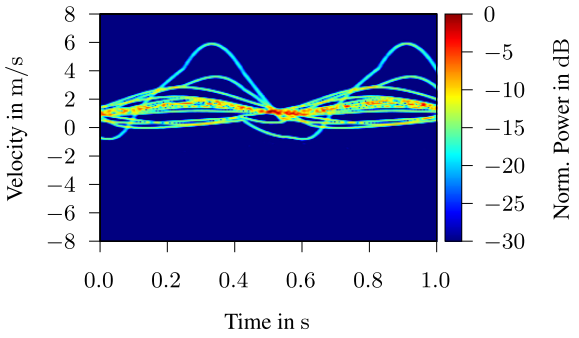

FIGURE 11. Velocity-time depiction of the generated input signal of the human walking model.

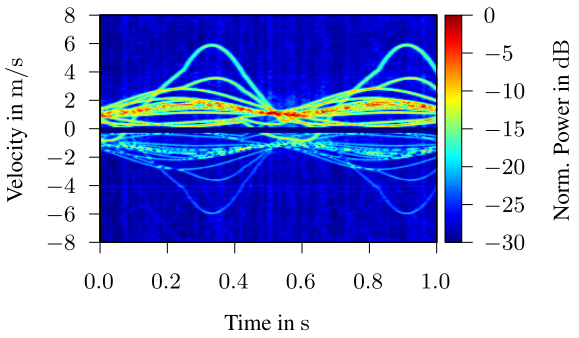

FIGURE 12. Velocity-time depiction of the replayed signal of the human walking model.

in this plot are also normalized to the maximum amplitude without including the zero-velocity information. Considering the amplitudes, there is a significant match of the amplitude as well as the velocity progress within the transmitted and received signal recognizable. However, the velocities get mirrored along the time axis and are suppressed by around −15 dB. This harmonic distortion is due to the RUT as it will be shown in the results of a measurement using the RUT without including the RTS setup. Furthermore, due to the measurement setup, a significant noise floor becomes noticeable in the rD plot. While the input signal showed a clear, noise-free signature, the result of the replay contains a noise floor that is suppressed by approximately −25 dB.

As stated earlier, also the replay of measured scenarios is possible with the presented setup. Fig. 13 shows the velocity-time result of a measured scenario using the RUT. In this scenario a person is running towards the radar. The increasing amplitude in the recorded signature indicates a person that is approaching the radar. Besides the signature of the target at −3 m/s, there is a constant velocity component at −4 m/s indicating a constant parasitic frequency. As mentioned, the frequency components get mirrored along the time axis and are detectable at 3.5 m/s and at 7 m/s. Also the parasitic frequency is slightly visible in the positive velocity region. These replicates indicate that there are harmonic distortions due to the RUT and not due to the RTS.

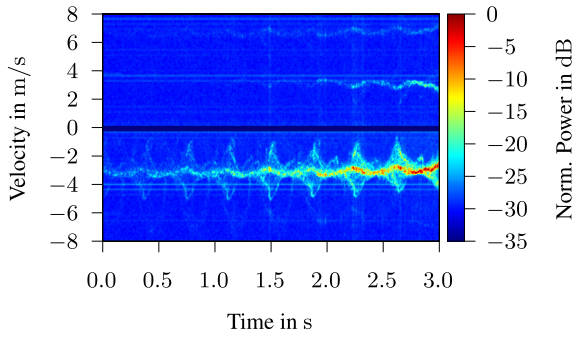

FIGURE 13. Velocity-time plot of a measurement of a running person.

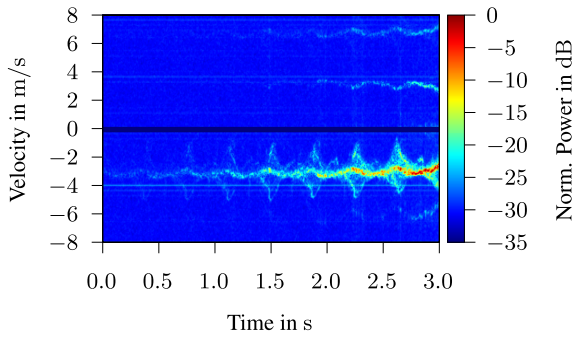

FIGURE 14. Velocity-time plot of a measurement of the replay of a running person.

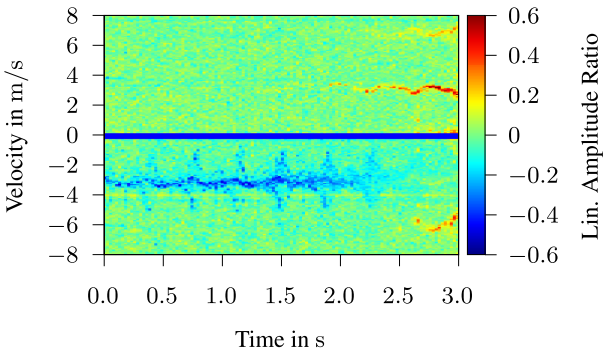

FIGURE 15. Lin. difference between the scenario measurement and recorded replay.

Fig. 14 depicts the result of the measured scene replayed by the RTS. The overall amplitude of the replayed scene is lower which is not compensated for illustration purposes. Thus the components in the beginning of the measurement are less visible compared to Fig. 13. However, the SNR of the replay approximately matches the SNR of the recorded scene. Regarding the signatures that were recorded, it can be stated, that any of them is present and clearly visible which also includes the parasitic components due to the RUT.

For the purpose of evaluating the quality of the replay, the difference between the RUT measured scenario and the RUT measured replay is depicted in Fig. 15. The difference plot is calculated by subtracting the information of the purely measured scenario from the replayed scenario measurement

while norming both maps to their maximum value. The result is afterwards divided by the corresponding bin values of the RTS map to receive a quality measure with respect to the original plot. This way, it becomes clear that for the replayed scenario the harmonic repetitions due to the RUT become stronger, while the signature of the person itself is weakened. This behavior indicates that the distortions due to the RUT add up such that the resulting measured signal exhibits these non-idealities even more compared to the pure measurement using the RUT once. Regarding the quality of the pure RTS replay, the signature of the person is replayed and measured correctly since the amplitude errors are small and thus neglectable for the generation of traffic scenarios.

This section set out how scenarios can be generated and replayed with the RTS setup. With the presented system and the target response generation, it is possible to represent any given range or range-velocity profile (within the limitations of the RUT chirp settings) with a radar signal model. Furthermore, there is also the possibility to directly simulate recorded measurements. The measured IF signals can either be recorded with a radar in CS-FMCW or CW mode. When measured in CW mode, a range has to be modulated onto the received IF signal in order to imitate a range profile for CS-FMCW configurations. With these options, it is possible to combine measurements and models into one target response that represents a scenario in the near range.

V. CONCLUSION

Summarizing the presented working principle, both the chirp-wise and the frame-wise signal generation method provide a practical solution in order to directly modulate the carrier signal of a CS-FMCW radar sensor. The main difference between the chirp-wise and the frame-wise approach is the sampling rate of the simulated target lists, and hence determines the desired accuracy of the scenario. Using the 2D-IFFT approach a fast conversion from rD data into corresponding IF signals is given. Furthermore, the usage of rD maps also includes the possibility to reproduce scenarios recorded with different radar settings and will thus be limited by the settings of the RUT. The chirp-wise approach facilitates the generation of IF signals given by simulations by sampling the scenario with the corresponding T_{RRI}.

The presented RTS with its working principle along with the signal generation methods provides a platform that allows radar sensors to be tested and evaluated. Especially considering the rising number of sensors that are required to enable highly automated or autonomous driving, the need for efficient testing environments becomes clear. In order to evaluate automotive radar sensors, the presented RTS can be used for the generation of arbitrary traffic scenarios and thus provides a test environment in order to reduce the amount of real world scenario testing.

ACKNOWLEDGMENT

The responsibility for the contents of this publication lies with the authors.

REFERENCES

[1] S. Kuutti, S. Fallah, K. Katsaros, M. Dianati, F. Mccullough, and A. Mouzakitis, "A survey of the state-of-the-art localization techniques and their potentials for autonomous vehicle applications," *IEEE Internet Things J.*, vol. 5, no. 2, pp. 829–846, Apr. 2018.

[2] J. Steinbäck, C. Steger, G. Holweg, and N. Druml, "Next generation radar sensors in automotive sensor fusion systems," in *Proc. Sensor Data Fusion, Trends, Solutions, Appl.*, 2017, pp. 1–6.

[3] I. Bilik, O. Longman, S. Villeval, and J. Tabrikian, "The rise of radar for autonomous vehicles," *IEEE Signal Process. Mag.*, vol. 36, no. 5, pp. 20–31, Sep. 2019.

[4] H. Winner and W. Wachenfeld, "Absicherung automatischen Fahrens," 6. FAS - Tagung, München, Nov. 2013.

[5] S. Lutz, C. Erhart, T. Walte, and R. Weigel, "Target simulator concept for chirp modulated 77 GHz automotive radar sensors," in *Proc. 11th Eur. Radar Conf.*, 2014, pp. 65–68. [Online]. Available: https://ieeexplore.ieee.org/document/6991208/

[6] M. Engelhardt, F. Pfeiffer, and E. Biebl, "A high bandwidth radar target simulator for automotive radar sensors," in *Proc. 13th Eur. Radar Conf.*, 2016, pp. 245–248.

[7] T. Dallmann, J. K. Mende, and S. Wald, "ATRIUM: A radar target simulator for complex traffic scenarios," in *Proc. IEEE MTT-S Int. Conf. Microw. Intell. Mobility*, 2018, pp. 1–4.

[8] W. Scheiblhofer, R. Feger, A. Haderer, and A. Stelzer, "A low-cost multi-target simulator for FMCW radar system calibration and testing," in *Proc. Eur. Radar Conf.*, 2017, pp. 343–346.

[9] J. Iberle, P. Rippl, and T. Walter, "A near-range radar target simulator for automotive radar generating targets of vulnerable road users," *IEEE Microw. Wireless Compon. Lett.*, vol. 30, no. 12, pp. 1213–1216, Dec. 2020.

[10] P. Schoeder, B. Schweizer, A. Grathwohl, and C. Waldschmidt, "Multitarget simulator for automotive radar sensors with unknown chirp-sequence modulation," *IEEE Microw. Wireless Compon. Lett.*, vol. 31, no. 9, pp. 1086–1089, Sep. 2021.

[11] D. J. Belgiovane and C. C. Chen, "Micro-Doppler characteristics of pedestrians and bicycles for automotive radar sensors at 77 GHz," in *Proc. 11th Eur. Conf. Antennas Propag.*, 2017, pp. 2912–2916.

[12] P. Rippl, J. Iberle, M. A. Mutschler, P. A. Scharf, H. Mantz, and T. Walter, "Analysis of pedestrian gait patterns using radar based micro-Doppler signatures for the protection of vulnerable road users," in *Proc. IEEE MTT-S Int. Conf. Microw. Intell. Mobility*, 2020, pp. 1–4.

[13] R. Boulic, N. M. Thalmann, and D. Thalmann, "A global human walking model with real-time kinematic personification," *Vis. Comput.*, vol. 6, no. 6, pp. 344–358, 1990.

[14] V. C. Chen, *The Micro-Doppler Effect in Radar*. Norwood, MA, USA: Artech House, 2011.

[15] P. Schoeder, V. Janoudi, B. Meinecke, D. Werbunat, and C. Waldschmidt, "Flexible direction-of-arrival simulation for automotive radar target simulators," *IEEE J. Microwaves*, vol. 1, no. 4, pp. 930–940, Oct. 2021.

[16] J. Iberle, M. A. Mutschler, P. A. Scharf, and T. Walter, "A radar target simulator for generating micro-Doppler-signatures of vulnerable road users," in *Proc. 16th Eur. Radar Conf.*, 2019, pp. 17–20.

[17] J. Iberle, M. A. Mutschler, P. A. Scharf, and T. Walter, "A radar target simulator concept for close-range targets with micro-Doppler signatures," in *Proc. German Microw. Conf.*, 2019, pp. 198–201.

[18] S. Z. Gurbuz, B. Tekeli, M. Yuksel, C. Karabacak, A. C. Gurbuz, and M. B. Guldogan, "Importance ranking of features for human micro-Doppler classification with a radar network," in *Proc. 16th Int. Conf. Inf. Fusion*, vol. 268-276, 2013, pp. 610–616.

PATRICK RIPPL (Graduate Student Member, IEEE) received the B.Sc. degree in mechatronics and robotics from the University of Applied Sciences Technikum Wien, Vienna, Austria, in 2014, the M.Eng. degree in system engineering from the University of Applied Sciences Ulm, Ulm, Germany, and the M.Sc. degree from the Rose Hulman Institute of Technology, Terre Haute, IN, USA, in 2019. He is currently working toward the Dr.-Ing. degree in the field of radar signal processing with the University of Applied Sciences Ulm, in cooperation with the Department of Microwave Engineering, University of Ulm. His research focuses on new approaches of classifying vulnerable road users and the simulation of traffic scenarios.

JOHANNES IBERLE (Student Member, IEEE) received the B.Eng. degree in communications engineering from the Ulm University of Applied Sciences, Ulm, Germany, in 2013, and the M.Sc. degree in electrical engineering from the Ulm University, in 2016. In 2016, he joined the Laboratory of Microtechnology, University of Applied Sciences, as a Research Assistant. His research interests include micro Doppler effects in radar and radar target simulators for automotive radar sensors.

PHILIPP A. SCHARF (Graduate Student Member, IEEE) received the B.Eng. degree in mechatronics from the Ulm University of Applied Sciences, Ulm, Germany, in 2013, and the M.Eng. degree in electrical engineering from the Constance University of Applied Sciences, Constance, Germany, in 2015. He is currently working toward the Dr.-Ing. degree with the Ulm University of Applied Sciences, in cooperation with the Institute of Microwave Engineering, Ulm University. His research interests include multi-band mmwave sensor applications and frequency-dependent scattering effects with focus on spectroscopic surface classification.

THOMAS WALTER (Member, IEEE) was born in 1963, Sigmaringen, Germany. He received the Diploma in electrical engineering and the Ph.D. degree for research on electrical defects in thin film semiconductors from Stuttgart University, Stuttgart, Germany, in 1990 and 1995, respectively. Afterwards, he joined Robert Bosch in Stuttgart, worked on microsystem technology, optical communication technology, and high-frequency electronics for automotive radars. During his Research and Development in industry, he was responsible for the introduction of SiGe-technology into 77 GHz radar sensors. In 2005, he joined the University of Applied Sciences Ulm, Germany, as a Professor for microtechnology. He conducts several research projects on thin film solar cells and microwave sensors. As a Student, he was granted a Scholarship from Studienstiftung des deutschen Volkes. During this time, he studied for one year with the University of Northumbria, Newcastle, U.K. In 2012, he was awarded the Wissenschaftspreis der Stadt Ulm for his research on microwave sensors. He is a reviewer of several IEEE journals in the field of microwaves and for MDPI journals in the field of thin film semiconductors.